# Coherent Motions in the Bottom Boundary Layer under Shoaling and Breaking Waves

Daniel T. Cox[1] and Nobuhisa Kobayashi[2]

**ABSTRACT:** Laboratory measurements of the instantaneous horizontal and vertical velocities induced by regular waves spilling on a rough, impermeable slope were analyzed to elucidate the nature of turbulence generated in the bottom boundary layer and by wave breaking. In the bottom boundary layer outside the surf zone, both the absolute shear stress $|\tau'|$ and the turbulent kinetic energy $k'$ exhibited intermittent behavior where the instantaneous values were often several times greater than the phase-averaged values. The motions occurred with the passing of each regular wave, however, and the phase-averaged values described the turbulent fluctuations reasonably well. A quadrant analysis showed that the turbulent velocities $u'$ and $w'$ were strongly correlated and oriented in either the first and third quadrants with $u'w' > 0$ during the acceleration phases or in the second and fourth quadrants with $u'w' < 0$ in the deceleration phase. The Reynolds stress contributions for this unsteady flow case depended strongly on the phase. Inside the surf zone, $|\tau'|$ and $k'$ were marked by intense, intermittent events which did not occur with the passing of each wave and which were roughly two orders of magnitude larger than the phase-averaged values. This intermittent motion extended into the wave bottom boundary layer. Near trough level, the intermittent events were phase-dependent, and the intense motion was primarily in the fourth quadrant. Near the bottom, the intermittent events were less phase-dependent. A preliminary analysis of the intensity and duration of the intermittent events indicated that coherent events occurred for about 10% of the record and accounted for approximately 50% of the motion, whereas intense events occurred for about 2% of the record and accounted for approximately 20% of the motion. These statistics clearly indicated that the intense, coherent events were intermittent and infrequent but contributed significantly to the magnitude of the absolute shear stress and turbulent kinetic energy.

## INTRODUCTION

Progress in understanding nearshore sediment suspension has been aided by the development of concentration sensors with high temporal resolution based on either optic or acoustic principles. Using these techniques, researchers have shown that nearshore sediment suspension is characterized by intermittent events and that these events, particularly inside the surf zone, can not be explained simply in terms of the free surface

[1]Asst. Prof., Ocean Engrg. Prog., Dept. of Civil Engrg., Texas A&M Univ., College Station, TX 77843-3136, USA; Email: dtc@arlo.tamu.edu; Tel: (409) 862 3627; Fax: (409) 862 8162.
[2]Prof. and Assoc. Dir., Center for Applied Coastal Res., Univ. of Delaware, Newark, DE 19716, USA; Email: nk@coastal.udel.edu; Tel: (302) 831 8044; Fax: (302) 831 1228.

elevation or local wave-induced horizontal velocity. A number of mechanisms have been put forward to explain the intermittent behavior of nearshore sediment suspension [e.g., *Jaffe et al.*, 1984; *Beach and Sternberg*, 1988; *Nadaoka et al.*, 1988; *Hanes*, 1991; *Hay and Bowen*, 1994]. Coherent fluid motions, such as bursting events in the boundary layer and large eddies produced by wave breaking, are plausible mechanisms but have received little attention due to a lack of suitable measurements, particularly estimates of the instantaneous vertical turbulent velocity, momentum flux and kinetic energy in the nearshore. In light of this, this paper identifies intermittent, coherent fluid motions under regular waves in three areas: (1) outside the surf zone and inside the bottom boundary layer where turbulence is generated at the boundary, (2) inside the surf zone in the interior region below trough level and above the bottom boundary layer where turbulence is generated primarily by wave breaking and (3) inside the surf zone and inside the bottom boundary layer where both mechanisms may be important. The term "bottom boundary layer" used in this paper is in reference to the wave bottom boundary layer which was shown to exist inside the surf zone [e.g., *Cox et al.*, 1996].

## EXPERIMENT

The nature of nearshore turbulence generated in the bottom boundary layer and by wave breaking is investigated using a laboratory flume since repeatability of the wave condition allows the turbulent signal to be extracted by phase-averaging. The experiment was conducted in a 33 m long, 0.6 m wide, and 1.5 m deep wave flume with a 1:35 impermeable slope, corresponding to a dissipative beach. A physical bottom roughness was added to the slope to increase the boundary layer roughness and boundary layer thickness so that the bottom boundary layer would be fully rough turbulent for non-breaking waves. The roughness was prepared by gluing sand grains with a median grain diameter of $d_{50} = 1.0$ mm to Plexiglas sheets and then taping these sheets over the entire slope. The adopted roughness in this small-scale experiment would correspond to gravel on a natural beach if geometric similitude were applied.

Six measuring lines were established, noted L1 to L6, and their cross-shore position relative to the spilling breakers can be described as follows: L1 was in the shoaling region seaward of breaking, L2 was at the break point defined as the onset of aeration in the tip of the wave crest, L3 was in the transition region where the wave changed from organized motion to a turbulent bore, and L4 to L6 were in the inner surf zone where the saw-toothed wave shape was a well-established turbulent bore. The free surface elevation, $\eta$, was measured at each measuring line using capacitance-type wave gages with a sampling rate of 100 Hz. The horizontal, cross-shore velocity, $u$, and the vertical velocity, $w$, were measured at a number of elevations at each measuring line by a fiber-optic laser-Doppler velocimeter (LDV). The effective sampling rate was in excess of $1 \times 10^3$ data points per second, and the data were reduced by band averaging to a sampling rate of 100 Hz. The flume was filled with fresh water to a depth of 0.4 m in the flat section of the tank, and regular waves were generated with a wave period of $T = 2.2$ s. Fifty regular waves were measured at each elevation, and the turbulent signal was extracted by phase-averaging.

Table 1 summarizes the measuring line locations and elevations. The second column indicates the horizontal coordinate, $x$, for each measuring line which is defined positive onshore with $x = 0$ at L1, where L1 was 9.8 m from the still water shoreline. The third

column indicates the depth $d$ below the still water level to the top of the Plexiglas sheet. The fourth column indicates the phase-averaged wave height $H$. The fifth column indicates the range of measuring elevations analyzed near the bottom with the number of elevations given in parenthesis. The vertical coordinate $z_m$ is defined positive upward with $z_m = 0$ on the bottom at each measuring line. The thickness of the wave bottom boundary layer is estimated to be approximately 1 cm based on the maximum shear velocity and angular wave frequency which is consistent with observations for this data set [*Cox et al.*, 1996].

Table 1: Measuring line locations and elevations.

| Line No. | $x$ (cm) | $d$ (cm) | $H$ (cm) | Range of $z_m$ (cm) analyzed BBL | | Interior | | Dropout Rate (%) |
|----|-----|-------|-------|-----------|-----|------------|------|----------|
| L1 | 0   | 28.00 | 13.22 | 0.20–1.10 | (7) | 1.60–24.10 | (10) | 0.6–2.1  |
| L2 | 240 | 21.14 | 17.10 | 0.20–1.10 | (7) | 1.60–16.10 | (8)  | 0.4–2.5  |
| L3 | 360 | 17.71 | 12.71 | 0.20–1.10 | (7) | 1.60–14.10 | (9)  | 0.3–8.6  |
| L4 | 480 | 14.29 | 8.24  | 0.20–1.10 | (7) | 1.60–12.10 | (8)  | 0.4–15.4 |
| L5 | 600 | 10.86 | 7.08  | 0.20–1.10 | (7) | 1.60–9.10  | (9)  | 0.6–3.1  |
| L6 | 720 | 7.43  | 5.05  | 0.20–1.10 | (7) | 1.60–6.10  | (6)  | 1.0–3.5  |

The sixth column indicates the range of measuring elevations in the interior region outside the bottom boundary layer to trough level with the number of elevations given in parenthesis. The seventh column indicates the range of the dropout rate for all elevations at each measuring line. The dropout rate is expressed as a percent and is typically low (less than about 2%), except near trough level for L3 and L4 due to aeration by the bores. Statistics presented in this paper were compared extensively using two types of time series, one in which the dropouts were excluded and a second in which the dropouts were replaced by a linear interpolation of the nearest points. For all elevations except those immediately below trough level at L3 and L4, there was no significant difference in the statistics using the two types of time series. In this paper, only the time series in which the dropouts were replaced by a linear interpolation are presented for clarity. As summarized in Table 1, the data set consists of a total of 86 measuring elevations from the bottom to trough level over six measuring lines. The following sections present the instantaneous and phase-averaged turbulence using three representative elevations: L2 at $z_m = 0.30$ cm inside the bottom boundary layer outside the surf zone, L5 at $z_m = 7.10$ cm in the interior region inside the surf zone, and L5 at $z_m = 0.30$ cm inside the bottom boundary layer inside the surf zone.

## INSTANTANEOUS AND PHASE-AVERAGED TURBULENCE

The instantaneous free surface elevation, $\eta$, and the horizontal and vertical velocities, $u$ and $w$, were phase-averaged over the fifty waves. The turbulent signals were defined as the difference of the instantaneous signals and phase-averaged signals and are expressed $\eta' = (\eta - \eta_a)$, $u' = (u - u_a)$, and $w' = (w - w_a)$ where the subscript $a$ denotes a phase-averaged quantity and the prime denotes a turbulent quantity. The phase-averaged quantities include both the organized wave-induced motion and the mean motion. The instantaneous turbulent momentum flux may be defined $\tau'/\rho = -u'w'$ where $\rho$ is the

fluid density and $\tau'_a$ is the phase-averaged Reynolds shear stress. The absolute value of the phase-averaged Reynolds shear stress, $|\tau'_a|$, is normally related to the concentration of suspended sediments at the bed or to the pick-up of bottom sediments. This approach may be reasonable if $|\tau'_a|$ represents most of the fluctuations in $|\tau'|$. The notation of $\tau' = -u'w'$ without the assumed constant $\rho$ is used in this paper for simplicity. The instantaneous turbulent kinetic energy per unit mass $k'$ is also of interest since it is not clear whether suspended sediments near the bed respond to $|\tau'|$ or $k'$. Since the cross-tank component of velocity, $v$, was not measured for this experiment, the turbulent kinetic energy per unit mass in this paper is defined as $k' = (u'^2 + w'^2)/2$ which is less than the actual $k'$ including the contribution of $v'^2$.

Figure 1 shows the temporal variations of the instantaneous and phase-averaged free surface elevation, horizontal and vertical velocities, absolute shear stress, and turbulent kinetic energy for L2 at $z_m = 0.30$ cm for $20 \leq t/T \leq 25$ where $t$ is time with $t = 0$ at the beginning of the 50 waves. The instantaneous and phase-averaged free surface elevation $\eta$ and $\eta_a$ in Figure 1a are difficult to distinguish and indicate the repeatability of the wave form. The wave shows strong asymmetry in both the horizontal and vertical planes. Figures 1b and 1c show the instantaneous and phase-averaged horizontal velocities, $u$ and $u_a$, and vertical velocities, $w$ and $w_a$. The phase-averaged horizontal velocity is dominant and much larger than the horizontal turbulent fluctuation. This assumption of a relatively weak turbulent intensity in a locally steady flow has been used in the analysis of surf zone turbulence [*George et al.*, 1994]. The phase-averaged vertical velocity $w_a$ is small at this elevation and throughout most of the water column except near trough level, and the vertical turbulent fluctuation is dominant $w'$ in comparison to $w_a$. Note that $u$ and $w$ were measured simultaneously and that the LDV and wave gage were synchronized to the wavemaker signal. Since multiple runs were repeated at the same measuring line, however, the velocity and free surface measurements presented in this figure and in Figure 2 are not synoptic.

Figures 1d and 1e show the instantaneous and phase-averaged variations of the absolute shear stress, $|\tau'|$ and $|\tau'|_a$, and turbulent kinetic energy, $k'$ and $k'_a$. Both $|\tau'|$ and $k'$ exhibit intermittent behavior where the instantaneous values are often several times greater than the phase-averaged values. Nevertheless, this motion occurs with the passing of each wave, and the phase-averaged values describe the turbulent fluctuations reasonably well with the following features: relatively low turbulence in the trough, an increase with the approaching wave crest (acceleration) which continues with the passing of the wave crest (deceleration). Elevations in the range $0.20 \leq z_m \leq 1.10$ cm exhibited similar behavior. Elevations for $z_m > 1.10$ cm above the bottom boundary layer outside the surf zone show very little turbulent motion [e.g., *Cox et al.*, 1994].

Figure 2 is similar to Figure 1 but for L5 inside the surf zone in the interior region at $z_m = 7.10$ cm where turbulence is generated by wave breaking. Comparison of $\eta$ and $\eta_a$ in Figure 2a shows the variability of the free surface inside the surf zone, particularly at the roller region on the crest of the wave. Inspection of the entire record $0 \leq t/T \leq 50$ did not reveal any large deviations in the instantaneous time series from the phase-averaged time series in the trough region, however. On the other hand, Figures 2b and 2c show intense, coherent motion in the horizontal and vertical velocities at $t/T \simeq 21$ and $t/T \simeq 24$. Inspection of the entire record $0 \leq t/T \leq 50$ for this elevation and for
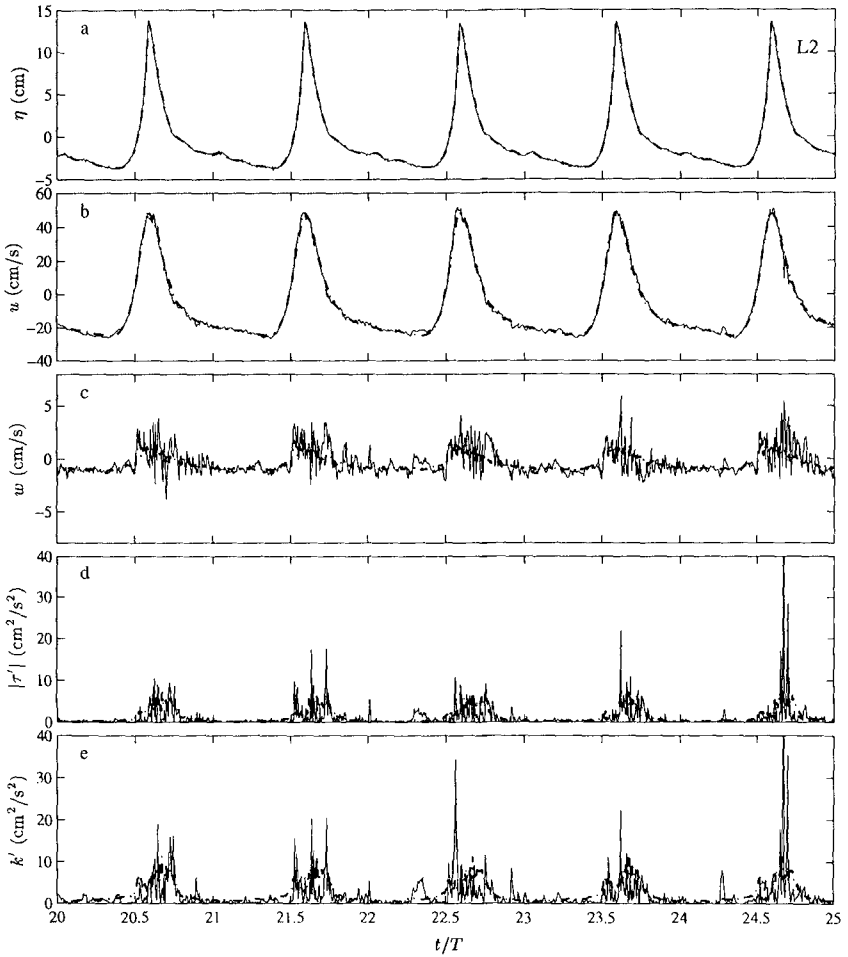
Figure 1: Temporal variation of (a) $\eta$, (solid) and $\eta_a$ (dash-dot); (b) $u$ (solid) and $u_a$ (dash-dot); (c) $w$ (solid) and $w_a$ (dash-dot); (d) $|\tau'|$ (solid) and $|\tau'|_a$ (dash-dot); and (e) $k'$ (solid) and $k'_a$ (dash-dot) in the range $20 < t/T < 25$ for L2 at $z_m = 0.30$ cm.

the other elevations inside the surf zone indicates that these intense turbulent events are intermittent, that they do not occur with the passing of each wave, and that the motions extends into the bottom boundary layer. The intense turbulent velocity fluctuations are of the same magnitude as the phase-averaged horizontal velocity, and the motion generally occurs with the passing of a wave crest and spreads downwards.

Figures 2d and 2e show the instantaneous and phase-averaged absolute shear stress and turbulent kinetic energy. Similar to L2, $|\tau'|$ and $k'$ are well correlated. However, $|\tau'|$ and $k'$ are an order of magnitude larger than in the bottom boundary layer outside the surf zone. Since the intense motion does not occur with each wave, this motion is more intermittent and can not be explained in terms of the phase-averaged quantities. In the bottom boundary layer inside the surf zone, the motion is characterized by intense, intermittent turbulence generated by wave breaking and less intense but more frequent turbulence generated at the boundary (Figure not shown).

Figures 3a–c show smoothed spectra of $k'$ and $k'_a$ at the representative locations. The spectral densities are plotted as a function of the frequency, $f*$, normalized by the wave period $T = 2.2$ s. The spectra of $k'_a$ were computed using phase-averaged time series repeated over 50 waves. All spectra were computed with detrended time series and were smoothed using band-averaging with 20 degrees of freedom. Figure 3a shows that the spectrum of $k'$ can be reasonably well represented by the spectrum $k'_a$, and that the low frequency components are small outside of the surf zone. Figure 3b shows that the spectrum of $k'_a$ describes a small portion of the $k'$ spectrum at the fundamental harmonic. Figure 3c shows that the spectrum $k'$ is poorly represented by the spectrum $k'_a$ inside the bottom boundary layer inside the surf zone. Figures 3b and 3c also show large low frequency components which are due to the intermittent nature of the eddies generated by wave breaking. The spectra for $|\tau'|$ and $|\tau'|_a$ are similar to those shown in Figure 3. These observations of small low frequency motion outside the surf zone and large low frequency motion inside the surf zone are consistent with observations of sediment suspension in a wave flume under regular waves [*Dally and Barkaszi*, 1994].

## QUADRANT ANALYSIS

In this section, a quadrant analysis is used to identify coherent motions in the instantaneous turbulent velocity time series. For unidirectional flow in the marine atmospheric boundary layer, *Boppe and Neu* [1995] used the quadrant technique to identify coherent motions and to quantify the bursting process. Associated with the bursting process are "ejections" where low speed fluid is brought up from the boundary layer and "sweeps" where high speed fluid rushes down from the outer layer. For unidirectional flow, motion in the second quadrant where $u' < 0$ and $w' > 0$ corresponds to ejections and motion in the fourth quadrant where where $u' > 0$ and $w' < 0$ corresponds to sweeps. Both ejections and sweeps contribute positively to the Reynolds stress since $\tau'/\rho = -u'w'$.

Figure 4 shows quadrant plots of $u'$ and $w'$ at 20 phases for the entire 50 waves in the range $0 \le t/T < 50$ for L2 at $z_m = 0.30$ cm. The time in the first quadrant for each panel indicates the phases for which the data were plotted. For example, $t_a/T = 0.05$ indicates that the data plotted in that panel correspond to all data in the range $0 \le t_a/T < 0.05$ over the fifty waves where $t_a/T$ is the normalized phase
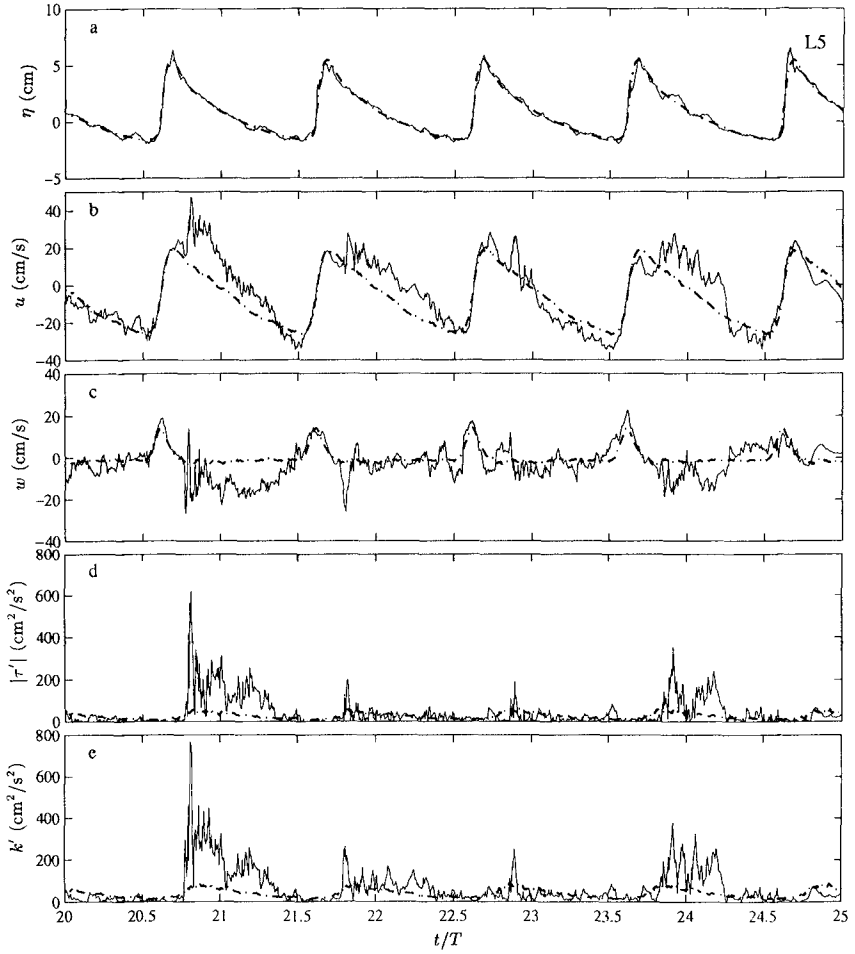
Figure 2: Same as Figure 1 for L5 at $z_m = 7.10$ cm.
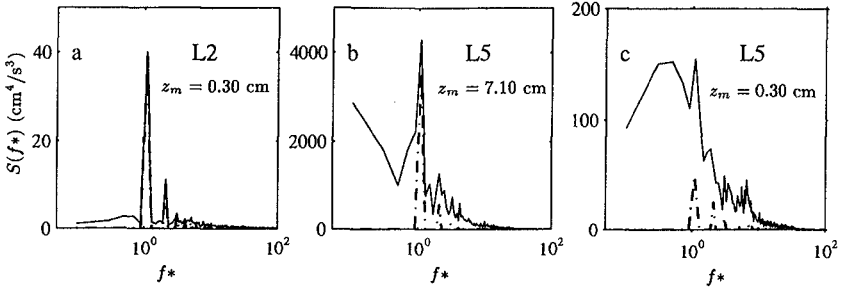
Figure 3: Spectral densities of $k'$ (solid) and $k'_a$ (dash-dot). NDOF = 20.

over one wave period. The four horizontal bars plotted along the vertical axis indicate (from top to bottom) the phase-averaged free surface elevation, $\eta_a$; the phase-averaged horizontal velocity, $u_a$; the local acceleration of the horizontal velocity, $\partial u_a / \partial t$; and the vertical gradient of the horizontal velocity $\partial u_a / \partial z$. The plotted values of $\eta_a$, $u_a$, $\partial u_a / \partial t$, and $\partial u_a / \partial z$ in each panel were averaged over that interval and were scaled by the maximum absolute value of the phase-averaged variable shown in the lower right of the figure. Temporal and spatial derivatives were estimated using a centered finite difference. The scaling is such that the maximum absolute value of the phase-averaged variable is equal to the upper limit of $u'$ on the abscissa of that figure. For example, $\eta_a = 13.5$ cm would correspond to $u' = 15$ cm/s in Figure 4. Although the phase-averaged variables may be difficult to interpret quantitatively in this figure, they give a useful qualitative comparison of the relative phases of these important variables.

In Figure 4, the top horizontal bar indicates that the wave crest occurs at $t_a/T = 0.65$, and the wave height decreases until reaching a minimum near $t_a/T = 0.40$. Comparison of the first and second bars indicates that $\eta_a$ and $u_a$ are generally in phase. The undertow is small compared to the maximum wave-induced velocity, $|\overline{u_a}|/|u_a|_{max} \simeq 0.14$. The third horizontal bar indicates that local deceleration of the flow starts at $t_a/T = 0.65$, is a minimum at $t_a/T = 0.70$, and deceleration continues until $t_a/T = 0.35$. At $t_a/T = 0.40$, the flow accelerates and reaches a maximum acceleration at $t_a/T = 0.55$. The bottom horizontal bar indicates that the vertical gradient of the horizontal velocity reaches a minimum at $t_a/T = 0.50$ and a maximum at $t_a/T = 0.70$. This gradient is large at this elevation compared to the elevations above the bottom boundary layer, and this gradient is not in phase with either the horizontal velocity or the local acceleration.

Figure 4 shows that the turbulent motion is most intense during periods of large local acceleration ($t_a/T = 0.55, 0.60$) and large local deceleration ($t_a/T = 0.65, 0.70, 0.75$). In the trough region, both the turbulent motion and the fluid acceleration is small. The horizontal and vertical velocity fluctuations are of similar magnitude and are generally much smaller than the phase-averaged horizontal velocity. Perhaps the most striking feature of Figure 4 is that the turbulent motion is strongly correlated and oriented in either the first and third quadrants with $u'w' > 0$ during the acceleration phases or in the second and fourth quadrants with $u'w' < 0$ in the deceleration phase.

This indicates that unidirectional flow results such as estimates of the Reynolds stress contributions can not be extended directly for oscillatory flow. The Reynolds stress contributions for this unsteady flow case depend strongly on the phase.

Similar to Figure 4, Figure 5 shows quadrant plots at 20 phases for L5 at $z_m = 7.10$ cm. The wave crest and maximum phase-averaged horizontal velocity occur at $t_a/T = 0.75$. The undertow is large, $|\overline{u_a}|/|u_a|_{max} \simeq 0.25$, and the vertical gradient of the horizontal velocity is small compared to L1 at $z_m = 0.30$ cm. The largest fluctuations of $u'$ and $w'$ occur after the passage of the wave crest and in the trough region $(t_a/T = 0.95, 0.95, 1.0, 0.05, 0.10, 0.15, 0.2)$. For the quadrant plots in this range, the large fluctuations occur primarily in the fourth quadrant, corresponding to sweeps where high speed fluid $(u' > 0)$ rushes downward $(w' < 0)$ due to wave breaking. The phase-averaged horizontal velocity is generally positive in this range $u_a > 0$, but because the undertow is strong, $u_a$ can become negative even when $\eta_a > 0$. The instantaneous values of $u'$ and $w'$ during sweeps can be as large as $|u_a|_{max} = 26.18$ cm/s in Figure 5.

## INTENSE COHERENT EVENTS

An analysis on the intensity and duration of the intermittent turbulent events is presented here similar to that by *Jaffe and Sallenger* [1992] for suspended sediments. Coherent events are defined in this paper when the magnitude of $|\tau'|$ or $k'$ exceeds a critical value. Since setting the critical values is somewhat subjective, the following procedure adopted from *Jaffe and Sallenger* [1992] was used. A coherent event was defined as $|\tau'| \geq (m + \sigma)$ where $m$ is the mean of $|\tau'|$ over the entire 50 waves at that elevation and $\sigma$ is the standard deviation. An intense event was defined as $|\tau'| \geq (m + 3\sigma)$. This analysis was also used to detect events in $k'$ where coherent events are defined as $k' \geq (M + \sigma_k)$ and intense events are defined as $k' \geq (M + 3\sigma_k)$ where $M$ is the mean and $\sigma_k$ is the standard deviation of $k'$ at that elevation. It is noted that the wave phase is not considered in this simplified analysis. Figure 6 illustrates the procedure with a portion $|\tau'|$ in the range $20 \leq t/T \leq 25$ for L5 at $z_m = 7.10$ cm. The lower dash-dot line shows the threshold $(m + \sigma)$ for the coherent events, and the upper dash-dot line shows the threshold $(m + 3\sigma)$ for the intense events. The corresponding detection of coherent events and intense events are shown by the solid lines above the $|\tau'|$ time series.

Statistics of coherent events and intense events for $|\tau'|$ and $k'$ were computed for all elevations listed in Table 1. Table 2 compares the statistics of $|\tau'|$ and $k'$ at L1 and L2 outside the surf zone. Statistics shown in this table are averages of the first four elevations near the bottom $z_m = 0.20, 0.25, 0.30$, and $0.40$ cm since these elevations were fairly similar in terms of $m$, $\sigma$, and $n_1/n$. In this table, $n_1$ is the number of coherent events out of a total number of data points, $n = 11000$, for which $|\tau'| \geq (m + \sigma)$; and $m_1$ is the average value of $|\tau'|$ for the coherent events. The second column essentially indicates the duration of the coherent event as a percent of the total record, $(n_1/n) \times 100$; and the third column indicates the percent of the motion contained in the coherent events in relation to that in the entire time series, $[(n_1 m_1)/(nm)] \times 100$. The subscript "3" indicates statistics computed using the definition of intense events, and the capital letters are used to distinguish coherent events and intense events computed using $k'$. In general, the statistics for the coherent events and intense events are similar for definitions based on $|\tau'|$ or $k'$. However, from L1 to L2, $(n_1 m_1)/(nm)$ and $(N_1 M_1)/(nM)$ are similar but $(n_3 m_3)/(nm)$ and $(N_3 M_3)/(nM)$ increase by approximately 15%, indicating

COASTAL ENGINEERING 1998
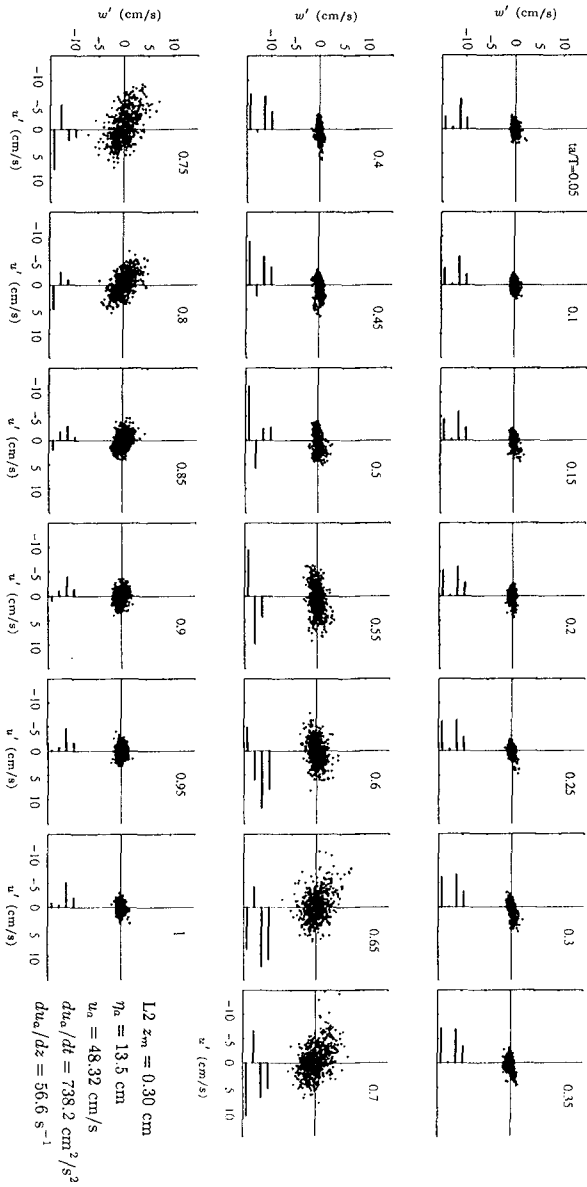


Figure 4: Quadrant plots at 20 phases for L2 at $z_m = 0.30$ cm. Figure explained in text.
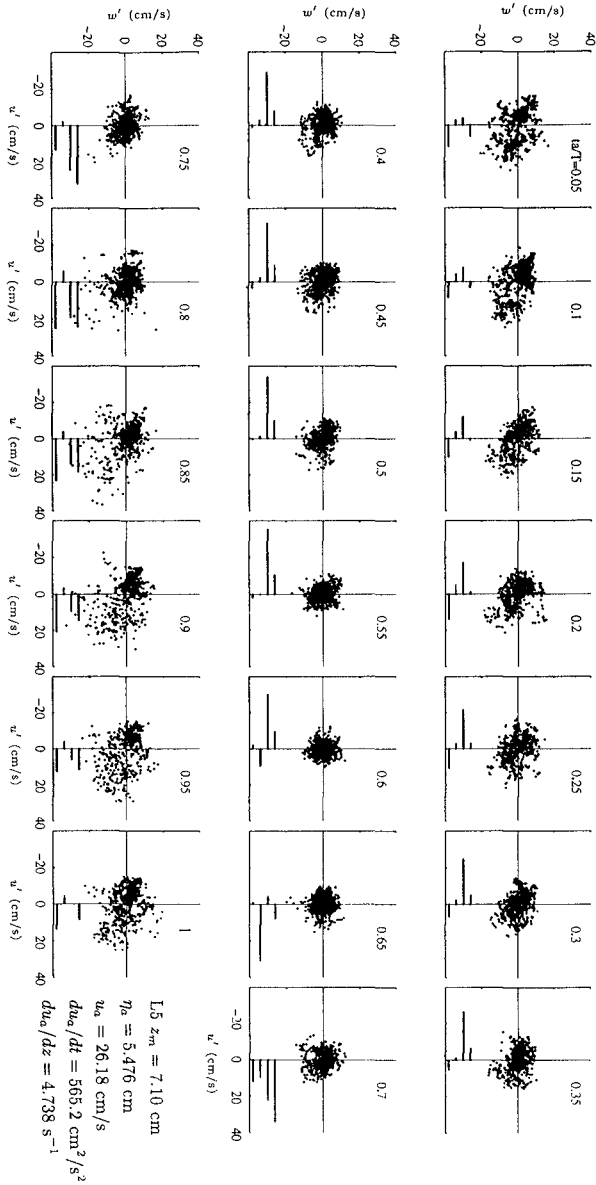
Figure 5: Same as Figure 4 for L5 at $z_m = 7.10$ cm.
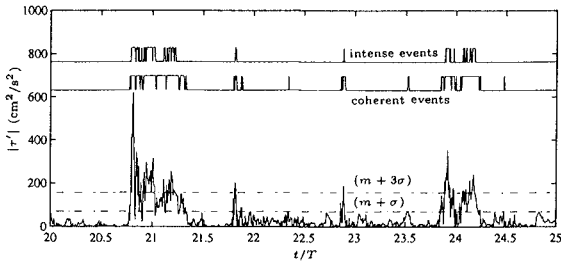
Figure 6: Detection of coherent events and intense events based on $|\tau'|$ for L5 at $z_m = 7.10$ cm.

Table 2: Coherent events and intense events detected using $|\tau'|$ and $k'$ for L1 and L2 averaged at each measuring line. Standard deviation in parenthesis

| Line | $|\tau'|$ | | | | $k'$ | | | |
|------|-----------|---|---|---|------|---|---|---|
| | Coherent Events | | Intense Events | | Coherent Events | | Intense Events | |
| No. | $\frac{n_1}{n}$ % | $\frac{n_1 m_1}{nm}$ % | $\frac{n_3}{n}$ % | $\frac{n_3 m_3}{nm}$ % | $\frac{N_1}{n}$ % | $\frac{N_1 M_1}{nM}$ % | $\frac{N_3}{n}$ % | $\frac{N_3 M_3}{nM}$ % |
| L1 | 8.6 (0.9) | 49.1 (0.6) | 1.9 (0.2) | 20.8 (2.3) | 10.0 (1.5) | 48.0 (0.6) | 2.1 (0.1) | 18.4 (3.4) |
| L2 | 6.9 (0.6) | 49.5 (4.6) | 1.8 (0.2) | 24.2 (2.6) | 8.1 (0.6) | 47.5 (4.4) | 1.9 (0.3) | 21.1 (2.1) |

that the magnitude of the intense events increases landward before breaking.

Table 3 lists the statistics of coherent events and intense events inside the surf zone. The statistics were averaged from $z_m = 0.20$ cm to trough level for all elevations at L3 to L6, and the standard deviations are given in parenthesis. The average statistics for L4, L5, and L6 in the inner surf zone are remarkably similar and suggest that it should be possible to parameterize the intense, coherent motion inside the surf zone. The average statistics for L3 in the transition region are different from those in the inner surf zone, and this suggests that the statistics could also vary with breaker type. Tables 2 and 3 shows that coherent events and intense events are of short duration, occuring for approximately 10% and 2% of the record, respectively, but contain a large portion of the turbulent motion, approximately 50% and 20%, respectively.

Table 3: Coherent events and intense events detected using $|\tau'|$ and $k'$ for L3 to L6 averaged at each measuring line. Standard deviation in parenthesis

| Line | $|\tau'|$ | | | | $k'$ | | | |
|------|-----------|---|---|---|------|---|---|---|
| | Coherent Events | | Intense Events | | Coherent Events | | Intense Events | |
| No. | $\frac{n_1}{n}$ % | $\frac{n_1 m_1}{nm}$ % | $\frac{n_3}{n}$ % | $\frac{n_3 m_3}{nm}$ % | $\frac{N_1}{n}$ % | $\frac{N_1 M_1}{nM}$ % | $\frac{N_3}{n}$ % | $\frac{N_3 M_3}{nM}$ % |
| L3 | 9.6 (1.3) | 44.5 (1.5) | 2.0 (0.2) | 17.4 (2.0) | 10.7 (1.4) | 42.8 (2.7) | 2.0 (0.2) | 14.4 (2.3) |
| L4 | 7.5 (1.3) | 43.7 (2.3) | 1.7 (0.3) | 19.6 (1.9) | 8.5 (1.7) | 42.4 (3.0) | 1.9 (0.4) | 18.1 (2.2) |
| L5 | 7.6 (1.1) | 43.5 (1.7) | 1.7 (0.3) | 19.5 (1.9) | 8.5 (1.8) | 41.1 (3.1) | 1.8 (0.4) | 17.1 (2.2) |
| L6 | 7.9 (0.8) | 43.5 (1.9) | 1.7 (0.2) | 19.1 (1.6) | 8.8 (1.3) | 41.8 (3.2) | 1.9 (0.4) | 17.0 (2.3) |

## CONCLUSIONS

In the bottom boundary layer outside the surf zone, the phase-averaged horizontal velocity is dominant and much larger than the horizontal turbulent fluctuation. The phase-averaged vertical velocity is small, and the vertical turbulent fluctuation is dominant. Both $|\tau'|$ and $k'$ exhibit intermittent behavior where the instantaneous values are often several times greater than the phase-averaged values. The motions occur with the passing of each regular wave, however, and the phase-averaged values described the turbulent fluctuations reasonably well. In the interior region below trough level inside the surf zone, the horizontal and vertical velocity records showed intense, intermittent turbulent events that did not occur with the passing of each wave. The intense turbulent fluctuations were of the same magnitude as the phase-averaged horizontal velocity. The instantaneous quantities of $|\tau'|$ and $k'$ could not be explained in terms of the phase-averaged quantities. The intermittent turbulent events extended into the bottom boundary layer inside the surf zone. The infrequent but intense turbulence generated by wave breaking is an order of magnitude larger than the turbulence generated locally at the boundary.

Spectra of $k'$ showed that the low frequency motion is small outside the surf zone and that the low frequency motion due to the intermittent turbulence from wave breaking increases inside the surf zone. Spectra of $k'$ are reasonably well represented by spectra of $k'_a$ outside the surf zone and poorly represented by spectra of $k'_a$ inside the surf zone. This conclusion was the same for the spectra of $|\tau'|$ and $|\tau'|_a$.

A quadrant analysis was used to show the relative contributions to the Reynolds stress as a function of wave phase. In the bottom boundary layer outside the surf zone, the turbulent motion was strongly correlated and oriented in either the first and third quadrants with $u'w' > 0$ during the acceleration phases or in the second and fourth quadrants with $u'w' < 0$ in the deceleration phases. In the interior region below trough level inside the surf zone, large fluctuations occurred primarily in the fourth quadrant, corresponding to sweeps where high speed fluid rushed downward due to wave breaking. These large motions did not occur with each wave but were phase-dependent near trough level. Near the bottom, the large motions were less dependent on phase and may be related to a more random arrival of eddies in the bottom boundary layer. The horizontal turbulent fluctuations increased relative to those outside the surf zone, whereas the vertical turbulent fluctuations were similar.

To analyze the intensity and duration of the intermittent turbulent events, two thresholds were used to distinguish coherent events and intense events. The analysis showed that coherent events occurred for about 10% of the record and accounted for approximately 50% of the turbulent motion. Intense events occurred for about 2% of the record and accounted for approximately 20% of the turbulent motion. These statistics indicated that coherent and intense events are infrequent but contribute significantly to the magnitude of $|\tau'|$ and $k'$ and possibly the suspension of bottom sediments.

These results are based on one experiment of regular laboratory waves spilling on a fixed, rough bottom. Further work with plunging waves, irregular waves, and movable beds will be necessary to generalize these conclusions. Nevertheless, this is an important step to show that instantaneous turbulence even for regular waves are dominated by

intense, intermittent events. Furthermore, this may explain difficulties in correlating suspended sediment concentrations and transport rates to phase-averaged or ensemble-averaged horizontal velocities. Parameterization and prediction of the intense events is left for further work but would likely be beneficial in developing predictive models for sediment suspension inside the surf zone.

## Acknowledgments

## REFERENCES

Beach, R.A., and R.W. Sternberg, Suspended sediment transport in the surf zone: Response to cross-shore infragravity motion, *Mar. Geol.*, 80, 61–79, 1988.

Boppe, R.S., and W.L. Neu, Quasi-coherent structures in the marine atmospheric surface layer, *J. Geophys. Res.*, 100 (C10), 20635–20648, 1995.

Cox, D.T., N. Kobayashi, and A. Okayasu, Vertical variations of fluid velocities and shear stress in surf zones, in *Proceedings of the 24th International Conference on Coastal Engineering*, 98–112, Am. Soc. Civ. Eng., New York, 1994.

Cox, D.T., N. Kobayashi, and A. Okayasu, Bottom shear stress in the surf zone, *J. Geophys. Res.*, 101 (C6), 14337–14348, 1996.

Dally, W.R., and S.F. Barkaszi, High-resolution measurements of sand suspension by plunging breakers in a large wave channel, in *Proceedings of Coastal Dynamics*, 263–277, Am. Soc. Civ. Eng., New York, 1994.

George, R.A., R.E. Flick, and R.T. Guza, Observations of turbulence in the surf zone, *J. Geophys. Res.*, 99 (C1), 801–810, 1994.

Hanes, D.M., Suspension of sand due to wave groups, *J. Geophys. Res.*, 96 (C5), 8911–8915, 1991.

Hay, A.E., and A.J. Bowen, Coherence scales of wave-induced suspended sand concentration fluctuations, *J. Geophys. Res.*, 99 (C6), 12749–12765, 1994.

Jaffe, B.E., and A.H. Sallenger, The contribution of suspension events to sediment transport in the surf zone, in *Proceedings of the 23rd International Conference on Coastal Engineering*, Am. Soc. Civ. Eng., 2680–2693, 1992.

Jaffe, B.E., R.W. Sternberg, and A.H. Sallenger, The role of suspended sediment in shore-normal beach profile changes, in *Proceedings of the 19th International Conference on Coastal Engineering.*, 1983–1996, Am. Soc. Civ. Eng., New York, 1984.

Nadaoka, K., S. Ueno, and T. Igarashi, Sediment suspension due to large scale eddies in the surf zone, in *Proceedings of the 21st International Conference on Coastal Engineering*, 1646–1660, Am. Soc. Civ. Eng., New York, 1988.